Mechanism of response of potential-sensitive dyes studied by time-resolved fluorescence

Tapan K. Das, N. Periasamy, and G. Krishnamoorthy
Chemical Physics Group, Tata Institute of Fundamental Research, Homi Bhabha Road, Bombay 400 005, India

ABSTRACT The mechanism of response of two potential-sensitive dyes, $diOC_2(5)$ (3,3'-diethyloxadicarbocyanine iodide) and oxonol V (bis-[3-phenyl-5-oxoisoxazol-4-yl]pentamethine oxonol), were studied by using steady-state and time-resolved fluorescence techniques. The lipid concentration dependence of the $\Delta\psi$ (membrane potential)-induced change in total fluorescence intensity was quite different for these two dyes. Time-resolved fluorescence measurements showed that the fluorescence decay of these dyes in membranes could be resolved into at least three exponentials. $\Delta\psi$-induced changes in the levels of these three populations were also measured under a variety of conditions. In the case of $diOC_2(5)$ an inside negative $\Delta\psi$ increased the levels of the bound forms. This shows that $diOC_2(5)$ responds to $\Delta\psi$ mainly by an "on–off" mechanism whereby $\Delta\psi$ perturbs the membrane–water partition coefficient of the dye. The $\Delta\psi$-induced changes approached zero when the dye was totally membrane bound. In contrast, the $\Delta\psi$-induced response of oxonol V increased with increased membrane binding. An inside negative $\Delta\psi$ decreased the level of the bound form with a longer lifetime. This shows that the mechanism of response of oxonol V is a $\Delta\psi$-induced shift in the equilibrium between bound forms of the dye.

INTRODUCTION

A large variety of dyes have been widely used in measuring transmembrane electrical potentials in cells, organelles, and vesicular systems (1–11). The absorbance and, in most cases, the fluorescence intensity of these dyes are sensitive to the membrane potential ($\Delta\psi$).[1] Such measurements using dyes are useful in situations where microelectrodes cannot be used. These dyes have been broadly classified into two types, i.e., "fast" and "slow" dyes based on their response time (1). Generally, fast dyes are associated with smaller changes in their signals (either fluorescence or absorbance changes). However, they are useful in real-time monitoring of rapidly changing $\Delta\psi$, as in the case of propagation of the action potential.

There have been a substantial number of models and experimental work (12–20) aimed at delineating the mechanism(s) by which these dyes respond to $\Delta\psi$. Understanding the mechanism(s) is essential in interpreting the observed signal changes. A variety of mechanisms have been proposed (12–20) to explain the response of these dyes. They can be classified broadly into the following four types.

"On–off" mechanism

In this mechanism (13, 19), the partitioning of the dye between the membrane phase and the aqueous phase is dependent on $\Delta\psi$. Because the quantum yield of these dyes is environment sensitive, the observed fluorescence intensity becomes $\Delta\psi$ sensitive. This mechanism is valid only for dyes with fixed charge(s) on them. According to this mechanism, the signal could be observed for either sign of $\Delta\psi$. Although the on–off mechanism is applicable to both membrane-permeable and impermeable dyes, it is more relevant to the latter (19). The response time, according to this mechanism, is generally well below 1 s (13, 19); hence the dyes that respond by this mechanism would be classified as fast dyes.

$\Delta\psi$-dependent equilibrium between membrane-bound dye populations

The dye populations within the membrane could be either in different orientations (such as parallel and perpendicular to the membrane plane), as shown in the case of merocyanine 540 (14), or at different locations within the membrane, as suggested in the case of some oxonols (20). Molecules with large permanent dipole moments such as these dyes could reorient within the membrane in the presence of $\Delta\psi$. These populations could have different quantum yields; hence the $\Delta\psi$-induced perturbations of the equilibrium could result in changes in the fluorescence intensity. These changes would be substantial if some of the populations are nonfluorescent, as in the case of dimers suggested for merocyanine 540 (14). Because $\Delta\psi$-induced reorientations take place within the membrane, the response time of these dyes would be even faster (μs–ms) than that expected for an on–off mechanism. Similarly to the on–off mechanism, this mechanism also would result in signal changes for either sign of $\Delta\psi$.

$\Delta\psi$-induced uptake of the dye

In this mechanism, the dyes that are permeant and having a permanent charge will distribute across the vesicular membrane in a Nernstian fashion. When the sign of

Address correspondence to Dr. G. Krishnamoorthy, Chemical Physics Group, Tata Institute of Fundamental Research, Homi Bhabha Road, Bombay 400 005, India.

[1] *Abbreviations used in this paper:* $diOC_2(5)$, 3,3'-diethyloxadicarbocyanine iodide; oxonol V, bis-[3-phenyl-5-oxoisoxazol-4-yl]pentamethine oxonol; $\Delta\psi$, membrane potential (inside vs. outside).

0006-3495/93/04/1122/11 $2.00

$\Delta\psi$ (inside versus outside) is opposite to that of the net charge on the dye, the dye will get concentrated in the inner aqueous phase, leading to concentration quenching of the fluorescence. Obviously, when the sign of $\Delta\psi$ is the same as the sign of the charge on the dye, there will be no change in the observed fluorescence intensity. Dyes responding by this mechanism are generally associated with much larger signal changes compared with the dyes that respond by the earlier mechanisms (1, 7). The process of translocation across the membrane makes the response time slow (s–min). Hence such dyes have been labeled as slow dyes (1).

Charge-shift electrochromic mechanism

The absorption spectrum of the dye molecule anchored in the membrane undergoes a perturbation caused by $\Delta\psi$ (21–23). Upon excitation, an electronic redistribution occurs in the dye molecule. If the direction of the resultant charge shift is perpendicular to the membrane plane (and hence parallel to $\Delta\psi$) the energy of the electronic transition is altered (24). Evidence for this mechanism has been provided in a few cases. Because the response does not involve any nuclear rearrangement, it is expected to be very fast ($\sim 10^{-13}$ s). Unlike the previous mechanism, this does not involve equilibrium among different populations.

Apart from such a generalization, a few other special mechanisms have also been proposed in some individual cases (25).

One of the major difficulties in discriminating between various mechanisms is the severe overlap of spectra (both absorption and emission) of the different dye populations mentioned above. In this work, we have resolved dye populations through their fluorescence decay kinetics. $\Delta\psi$-induced changes in these population levels were inferred from the changes in the amplitudes of their time-resolved fluorescence intensities. Our results show that the dye $diOC_2(5)$ (3,3′-diethyloxadicarbocyanine iodide) works by an on–off mechanism (type 1); in the case of oxonol V (bis-[3-phenyl-5-oxoisoxazol-4-yl]-pentamethine oxonol), the response mainly comes from a $\Delta\psi$-dependent shift in the equilibrium between bound forms (type 2).

MATERIALS AND METHODS

Sonicated soybean phospholipid vesicles (26) were used in most of the experiments. $DiOC_2(5)$ and oxonol V were obtained from Molecular Probes Inc. (Eugene, OR).

Steady-state fluorescence measurements were carried out using a spectrofluorophotometer (model RF 540; Shimadzu Corp., Kyoto, Japan). Fluorescence lifetimes were measured using a CW mode-locked Nd-YAG laser-driven dye (Rhodamine 6G) laser system described elsewhere (27). Fluorescence decay curves were obtained using a time-correlated single photon counting set-up (27) coupled to a microchannel plate photomultiplier (model 2809U; Hamamatsu Corp.). The halfwidth of the excitation response function was ~100 ps (28).

The samples were excited with (typically) 4-ps pulses from the dye laser and the fluorescence emission was collected through either a 590-nm (in the case of $diOC_2[5]$) or a 630-nm (in the case of oxonol V) cut-off filter followed by a monochromator. The cut-off filter was necessary because of high levels of scattering of the excitation beam from liposome suspensions. The effectiveness of this step was checked in control experiments in liposome suspensions in the absence of the dye. The peak counts obtained in control experiments were comparable to the background level. In fluorescence lifetime measurements, the emission was monitored at the magic angle (54.7°) to eliminate the contribution from the decay of anisotropy. In time-resolved anisotropy measurements, the emission was collected at directions parallel ($I_\parallel$) and perpendicular ($I_\perp$) to the polarization of the excitation beam. The anisotropy (r) was calculated as:

$$r(t) = \frac{I_\parallel - I_\perp \cdot G(\lambda)}{I_\parallel + 2I_\perp \cdot G(\lambda)},$$

where $G(\lambda)$ is the geometry factor at the wavelength (λ) of emission. The G factor of the emission collection optics was determined in separate experiments using a standard sample ($diOC_2(5)$ in buffer).

The fluorescence decay curves at the magic angle were analyzed by deconvoluting with the excitation function (obtained using a purely scattering medium) to obtain the intensity decay function represented as a sum of three exponentials:

$$I(t) = \sum_i A_i \exp(-t/\tau_i), \quad i = 1, 2, 3.$$

Nonlinear least square analysis (Marquardt method) was performed to extract the amplitude parameters A_i and the lifetimes τ_i (29). In most of the cases, pairs of decay curves (obtained in the presence and in the absence of $\Delta\psi$) were analyzed globally (30). Such analyses fit the two decay curves with the same values of τ_i but with different values of A_i. This was essential to get unambiguous information of the $\Delta\psi$-induced change in the value of A_i, which was often very small (see Results). Global analysis of more than two decay curves was performed in experiments designed to obtain the variation of A_i with the concentration of lipid.

The experiments were performed at 23–25°C. Other experimental conditions are given in the figure legends.

RESULTS

We have selected the positively charged dye $diOC_2(5)$ and the negatively charged dye oxonol V as typical candidates for our studies. These dyes have been used in a large number of experiments (e.g., 5, 25, 31–35).

Steady-state fluorescence measurements

The steady-state fluorescence of both $diOC_2(5)$ and oxonol V in liposome suspensions was sensitive to $\Delta\psi$ (Fig. 1). $\Delta\psi$ was generated as valinomycin-induced K^+ diffusion potential (see legend to Fig. 1). An inside negative $\Delta\psi$ increased the fluorescence intensity in the case of $diOC_2(5)$ and decreased the intensity in the case of oxonol V. Opposite effects were observed when the polarity of $\Delta\psi$ was reversed (Fig. 1). These changes are similar to those observed by others (5, 20, 27). Valinomycin-induced fluorescence changes changed sign when the sign of $\Delta\psi$ was reversed (Fig. 1). This was also seen in the amplitude parameters ΔA_i obtained from time-resolved fluorescence data (see below). These show that the ob-

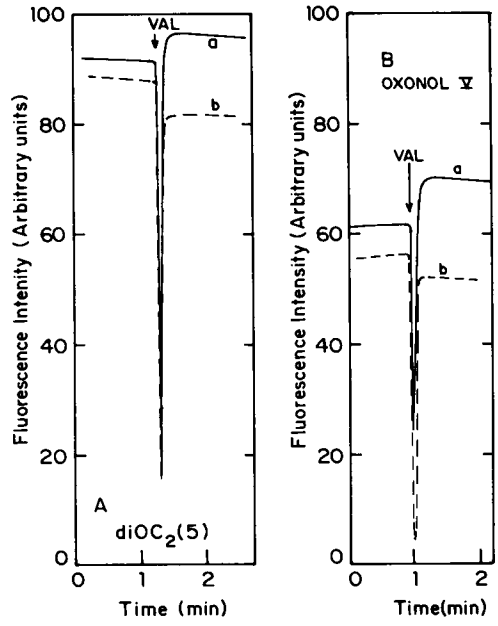

FIGURE 1 $\Delta\psi$-induced changes in fluorescence intensity. (*A*) $diOC_2(5)$; trace *a*, $\Delta\psi$ is negative: to a suspension of soybean phospholipid vesicles (0.69 mg/ml) in 150 mM NaCl, 4.5 mM KCl, 30 mM NaH_2PO_4, 2×10^{-7} M $diOC_2(5)$, pH 7.5, valinomycin (2×10^{-7} M) was added. The buffer composition in the inner aqueous phase was 150 mM KCl, 30 mM KH_2PO_4, pH 7.5. The magnitude of $\Delta\psi$ generated by valinomycin-induced K^+ diffusion potential, calculated from the Nernst equation, is −89.8 mV. The excitation was at 575 nm and the fluorescence intensity was measured at 630 nm. The downward spike is due to opening and closing of the sample compartment. Trace *b*, $\Delta\psi$ is positive: the internal buffer was 150 mM NaCl, 3 mM KCl, 30 mM NaH_2PO_4, pH 7.5, and the external buffer was 150 mM KCl, 30 mM KH_2PO_4, pH 7.5. (*B*) Oxonol V: trace *a* was for $\Delta\psi$ positive and the trace *b* was for $\Delta\psi$ negative. The concentrations of oxonol V and the lipid were 5×10^{-7} M and 0.38 mg/ml, respectively. The fluorescence was monitored at 650 nm by exciting at 600 nm.

served fluorescence changes were caused by $\Delta\psi$ rather than by any interaction of valinomycin with the dye. Furthermore, the low levels of valinomycin (whose final concentration was <1/50th of the concentration of the dye) used in our experiments are unlikely to have caused significant levels of complex formation with the dye. Furthermore, $\Delta\psi$-induced fluorescence changes were also observed when $\Delta\psi$ was generated by a ΔpH-induced H^+ diffusion potential (data not shown). The normalized fluorescence intensity changes, $\Delta F/F$, induced by $\Delta\psi$ decreased with increasing concentration of the lipid in the case of $diOC_2(5)$ (Fig. 2 *A*). In contrast, in the case of oxonol V, $\Delta F/F$ showed an initial sharp increase followed by a slight decrease (Fig. 2 *B*). Fig. 2, *A* and *B*, also show the titration of the total fluorescence intensity with the concentration of lipid. These titrations show that the binding of both the dyes to the liposome is essentially complete beyond ~1 mg/ml of lipid (Fig. 2, *A* and *B*). Taken together, these results suggest that the two dyes respond to $\Delta\psi$ by different mechanisms. In the case of $diOC_2(5)$, $\Delta F/F$ decreased with increased binding to liposomes and essentially approached to zero when the binding is complete. In contrast, in the case of oxonol V, $\Delta F/F$ showed an increase with increased binding. Furthermore, the signal change, $\Delta F/F$, remained substantial even when the dye binding to liposomes was essentially complete (Fig. 2 *B*).

Time-resolved fluorescence measurements

To get a clear understanding of the mechanism of response of these dyes, time-resolved fluorescence mea-

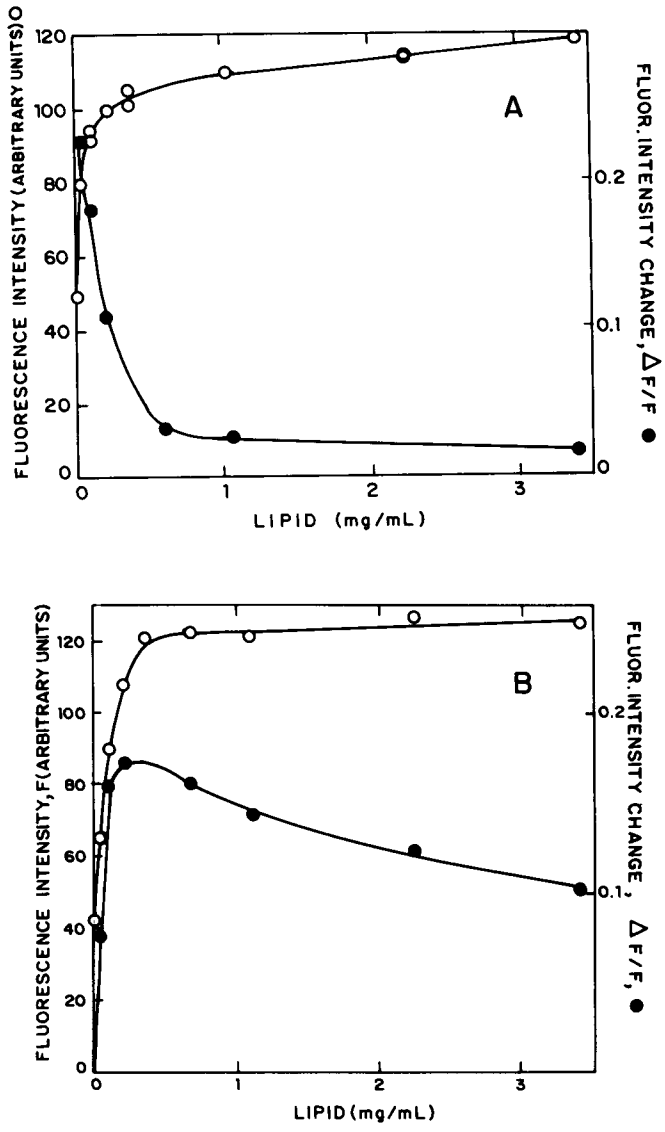

FIGURE 2 Lipid concentration dependence of the fluorescence intensity and $\Delta\psi$-induced intensity changes. (*A*) $diOC_2(5)$: the fluorescence intensity (○) was measured at 630 nm in a medium containing 150 mM NaCl, 30 mM NaH_2PO_4, pH 7.5. The concentration of $diOC_2(5)$ was 6×10^{-7} M. The residual scattering due to liposome suspension has been corrected for in these data (○). $\Delta\psi$-induced intensity changes (●) were measured for $\Delta\psi$ negative inside. (*B*) Oxonol V: the fluorescence intensity (○) was measured at 650 nm in a medium containing 150 mM NaCl, 30 mM NaH_2PO_4, pH 7.5. The concentration of oxonol V was 10^{-6} M. $\Delta\psi$-induced changes in the fluorescence intensity (●) were measured in situations where the $\Delta\psi$ was positive inside.

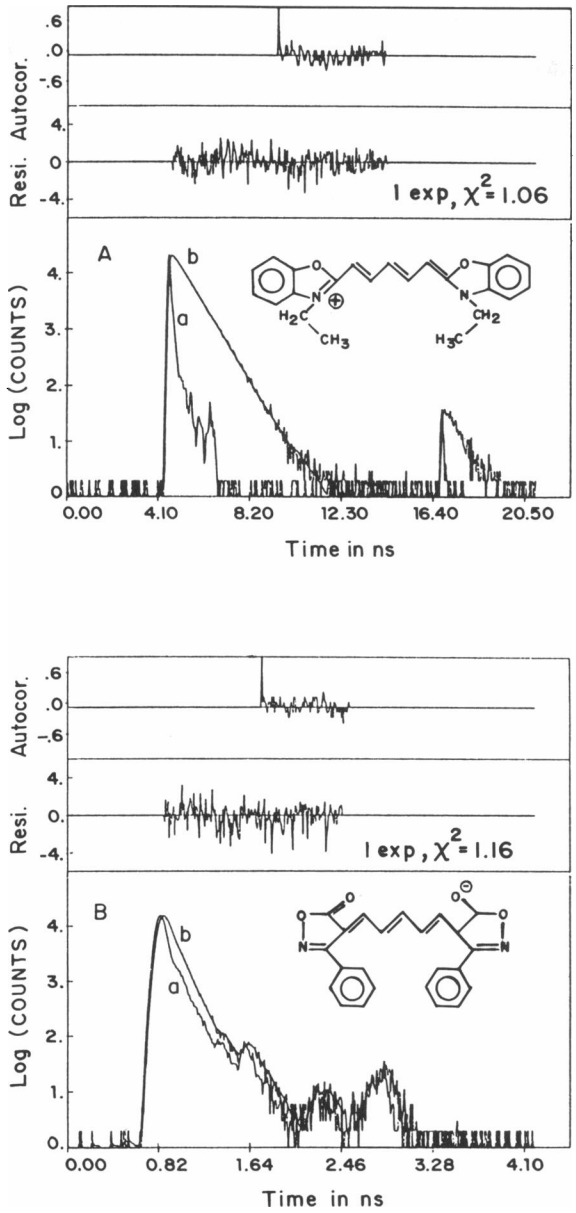

FIGURE 3 Fluorescence decay of $diOC_2(5)$ (*A*) and oxonol V (*B*) in buffer (150 mM KCl, 30 mM KH_2PO_4, pH 7.5). The excitation profile (*a*), emission profile (*b*), and the single exponential fit of the emission profile (*smooth line* in *b*) are shown. The residuals and the autocorrelations are given in *top panels*. The excitation and emission wavelengths were 575 and 590 nm for $diOC_2(5)$ and 600 and 630 nm for oxonol V. The time resolution was 41.6 ps/channel in *A* and 8.3 ps/channel in *B*. The deconvoluted fluorescence lifetimes were 650 ± 2 and 47 ± 1 ps, respectively.

surements were undertaken. Both $diOC_2(5)$ and oxonol V showed single fluorescence lifetimes in aqueous buffers. The lifetimes were 650 and 50 ps for $diOC_2(5)$ and oxonol V, respectively (Fig. 3 and Table 1). The fluorescence decay of both the dyes became multiexponential in the presence of soybean phospholipid vesicles. The decay curves could be fitted well to a sum of three exponentials (Fig. 4 and Table 1). In both the cases, biexponential fits were not satisfactory, as seen in the residuals (Fig. 4) and the values of χ^2. The three exponential time constants were ~0.6 (τ_1), 0.1 (τ_2), and 1.8 ns (τ_3) in the case of $diOC_2(5)$ and ~50 (τ_1), 0.3 (τ_2), and 0.6 ns (τ_3) in the case of oxonol V in a suspension of soybean liposomes. The relative contributions (A_1, A_2, and A_3) of the three lifetimes were dependent on the emission wavelength, λ_{em}. In the case of $diOC_2(5)$, A_1 and A_2 had a similar dependence on λ_{em}. A_2 and A_3 showed similar dependence in the case of oxonol V (data not shown).

$diOC_2(5)$

In the case of $diOC_2(5)$, one of the three lifetimes (τ_1 ~ 0.6 ns) obtained was not significantly far off from the lifetime obtained in the buffer alone. This indicates that τ_1 represents the dye population in the aqueous phase, and τ_2 and τ_3 represent the populations bound to the membrane. This conclusion was supported by a series of experiments in which the concentration of lipid was varied at a fixed concentration of the dye. In such titrations, the amplitude A_1 corresponding to τ_1 decreased with increasing concentrations of the lipid, whereas A_2 and A_3 (corresponding to τ_2 and τ_3, respectively) increased with increasing concentration of the lipid (Fig. 5 *A*). These changes are very similar to the changes of total fluorescence intensity with the concentration of lipid (Fig. 2 *A*). The lifetimes, however, were not significantly dependent on the concentration of the lipid (Fig. 6 *A*). Thus, these data support the model that τ_2 and τ_3 represent the membrane-bound dye, and τ_1 represents the free dye. (However, it should be noted that A_1 values, despite its decrease, did not approach zero at high concentration of the lipid [Fig. 5 *A*]. This would indicate that beyond ~1 mg/ml of lipid, the population with lifetime ~ 0.6 ns represents another bound form.) Neither A_i nor τ_i (i = 1, 2, 3) were significantly dependent on the concentration of the dye (in the range 0.05–1.0 μM) at a fixed concentration of lipid (data not shown).

The imposition of $\Delta\psi$ resulted in significant changes in the fluorescence decay profile. Analysis of a large number of decay profiles individually showed that none of the three lifetimes was significantly affected by $\Delta\psi$ (data not shown). However, the amplitudes A_i showed definite changes in the presence of $\Delta\psi$. Because these changes were quite small, especially at high concentrations of lipid, the decay profiles in the absence and in the presence of $\Delta\psi$ were analyzed globally in pairs (see Materials and Methods). In this analysis, the two decay profiles were simultaneously analyzed for the same set of τ_i but varying amplitudes A_i (30). Table 1 shows some typical results of such global analysis of pairs of decay curves. The results clearly show that $\Delta\psi$ perturbs the position of equilibrium between the free (A_1) and membrane-bound (A_2 and A_3) $diOC_2(5)$ populations. An inside negative $\Delta\psi$ decreased A_1 and increased both A_2 and A_3, showing an increased partitioning of the positively charged $diOC_2(5)$ into the membrane. $\Delta\psi$-induced

TABLE 1 **Fluorescence lifetimes (τ_i) and amplitude factors (A_i) of diOC$_2$(5) and oxonol V in liposome suspensions**

No.	Sample	$\Delta\psi$[§]	Fluorescence lifetime[‖]			Normalized amplitude factor[‖]			χ^2
			τ_1	τ_2	τ_3	A_1	A_2	A_3	
			ns						
1	diOC$_2$(5) in buffer*	—	0.65	—	—	1.0	—	—	0.99
2	diOC$_2$(5) in liposomes (0.11 mg/ml)[‡]	0	0.70	0.124	1.71	0.513	0.256	0.231	1.19
3	—do—	—	0.70	0.124	1.71	0.321	0.307	0.373	1.01
4	diOC$_2$(5) in liposomes (1.1 mg/ml)[‡]	0	0.56	0.101	1.76	0.316	0.230	0.456	1.17
5	—do—	—	0.56	0.101	1.76	0.238	0.295	0.467	1.29
6	diOC$_2$(5) in liposomes (1.1 mg/ml)[‡]	0	0.63	0.133	1.77	0.307	0.242	0.451	1.25
7	—do—	+	0.63	0.133	1.77	0.416	0.161	0.424	1.19
8	Oxonol V in buffer*	—	0.050	—	—	1.0	—	—	1.16
9	Oxonol V in liposomes (0.66 mg/ml)[‡]	0	0.041	0.269	0.649	0.414	0.386	0.200	1.15
10	—do—	+	0.041	0.269	0.649	0.404	0.356	0.240	1.20
11	Oxonol V in liposomes (0.66 mg/ml)[‡]	0	0.041	0.211	0.569	0.350	0.379	0.271	1.18
12	—do—	—	0.041	0.211	0.569	0.363	0.395	0.242	1.23
13	Oxonol V in liposomes (1.1 mg/ml)[‡]	0	0.056	0.304	0.689	0.391	0.424	0.185	1.35
14	—do—	+	0.056	0.304	0.689	0.387	0.387	0.226	1.33

* The buffer used was 150 mM NaCl, 30 mM NaH_2PO_4, pH 7.5.
‡ Data analyzed globally in pairs ($\Delta\psi = 0$ and $\Delta\psi \neq 0$.)
§ Membrane potential (inside versus outside).
‖ The standard deviations associated with the parameters are ~3%, except in the cases of A_1 and τ_1 associated with oxonol V, where the standard deviations were ~10%.

changes in A_i values showed a dependence on the concentration of lipid (Fig. 7 *A*). The magnitude of ΔA_i decreased with the increase in the lipid concentration and tended toward zero beyond ~1 mg/ml of lipid. These changes are similar to the lipid concentration dependence of the change in fluorescence intensity $\Delta F/F$, which also approached zero beyond ~1 mg/ml of lipid (Fig. 2 *A*). Also, the $\Delta\psi$-induced relative changes in the mean lifetime ($\tau_m = \sum_i A_i\tau_i$) agreed with $\Delta F/F$ values reasonably well. This shows that the response ($\Delta F/F$) of the observed fluorescence intensity to $\Delta\psi$ is due to the $\Delta\psi$-induced change in the partition of the dye between the aqueous and the membrane phases. Such a conclusion is supported by the steady-state measurements (Fig. 2, *A* and *B*), which showed negligible signal ($\Delta F/F$) when the dye was almost completely bound. In contrast to the shift in equilibrium between the free (A_1) and bound (A_2 and A_3) forms, there was no significant $\Delta\psi$-induced perturbation of the equilibrium between the two bound forms. $\Delta A_2/A_2$ and $\Delta A_3/A_3$ were of the same sign and of similar magnitudes (Table 1 and Fig. 7). Also, $\Delta A_2/A_2$ and $\Delta A_3/A_3$ decreased with increasing concentrations of the lipid, supporting the above conclusion.

Oxonol V

As mentioned earlier, the fluorescence decay of oxonol V in liposomes also could be fitted to a sum of three exponentials (Table 1). In this case also, a component, τ_1 (~50 ps), was found that is close to that of the free oxonol V (50 ps). In lipid titrations the amplitude (A_1) corresponding to τ_1 saturated at ~0.4 (Fig. 5 *B*), indicating that this component is bound at high lipid concentrations. Also, in titrations with lipid concentrations (Fig. 2 *B*), the total fluorescence intensity saturated beyond ~0.3 mg/ml, similar to earlier observations (25). This shows clearly that beyond ~0.3 mg/ml of lipid, the concentration of free dye is negligible. Hence, τ_1 obtained beyond ~0.3 mg/ml of lipid should represent a bound form similar to the observations with diOC$_2$(5). In the case of oxonol V in liposomes, the relative amplitudes A_i were dependent upon whether the analysis was performed on the complete decay curve (including the raising edge) or from the peak. Because the lifetime of free oxonol V is very short (50 ps), its decay information is contained in only a few initial channels. Hence the analysis was performed on the full decay curve so as to get the total information on the free form. The full curve analysis gave larger values of χ^2 (~1.5). However, τ_i values were very similar in both "full curve" and "from the peak" analysis. τ_1 and τ_2 were largely independent of the lipid concentration (Fig. 6 *B*). The longest lifetime τ_3 increased with increase in the concentration of the lipid. This could be due to concentration

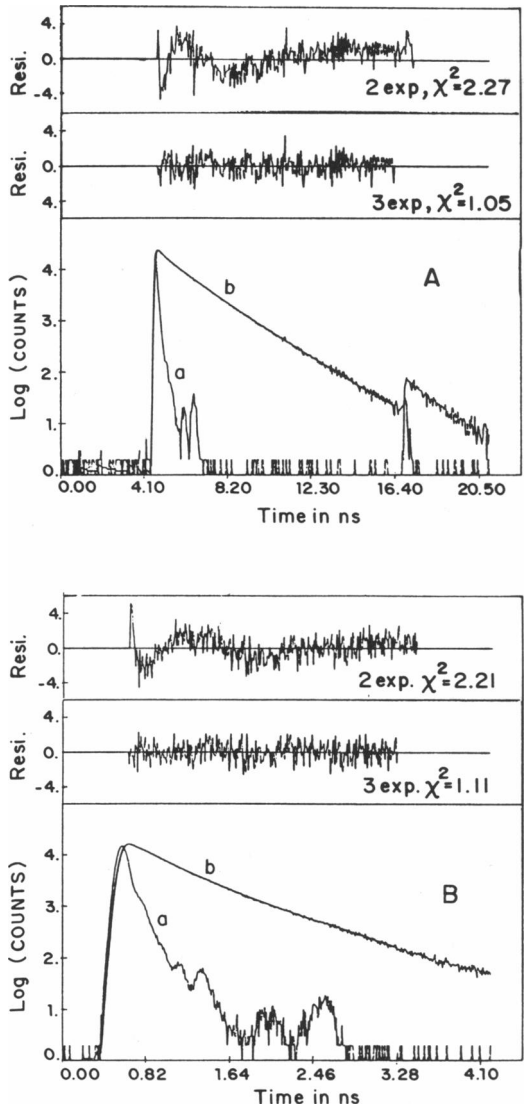

FIGURE 4 Typical fluorescence decay of $diOC_2(5)$ (*A*) and oxonol V (*B*) in liposome suspensions (1.1 mg/ml) in the absence of membrane potential. Traces *a* and *b* are excitation and emission profiles, respectively. Fits using a sum of three exponentials are given as smooth lines in *b*. The excitation and emission wavelengths were 575 and 590 nm for *A* and 600 and 630 nm for *B*. The parameters obtained by three exponentials fits are given in Table 1.

quenching of the dye at very low concentration of the lipid where concentration of the dye in the lipid would be high.

Generation of an inside positive $\Delta\psi$ resulted in an increase in A_3 and a decrease in A_2 (Table 1 and Fig. 7 *B*). The opposite effect was observed for an inside negative $\Delta\psi$. Because of low value of τ_1 the uncertainty in the measurement of A_1 is large ($\sim$10%). Hence small changes (<10%) in A_1 were not reliably obtained. However, inspection of a large number ($\sim$40) of sets of data show that in $\sim$70% of the cases, the sign of ΔA_1 was the same as that of ΔA_2. Another significant observation is that ΔA_i values did not approach zero with increase in the concentration of lipid but remained largely insensitive (Fig. 7 *B*). This is similar to the steady-state results (Fig. 2 *B*), where a significant amount of signal ($\Delta F/F$) was observed even when the dye was totally bound. This rules out an "on–off" mechanism, which would require a substantial reduction in the magnitude of ΔA_i with increasing concentration of lipid as observed in the case of $diOC_2(5)$. Also, this indicates a mechanism involving $\Delta\psi$-dependent shift in the equilibrium between bound forms, represented by τ_2 and τ_3 (type 2 mechanism). An inside positive $\Delta\psi$ would increase the population represented by τ_3 at the cost of the population represented by τ_2.

Time-resolved anisotropy measurements

Fig. 8 shows the decay of fluorescence anisotropy of the dyes in liposome suspensions. The aim of these measurements was to look for any $\Delta\psi$-dependent change in the dynamics of membrane-bound dyes. Hence, the fluorescence anisotropy was monitored at 610 nm, the wavelength where the emission from the free form is less predominant, in the case of $diOC_2(5)$, and at 630 nm in the case of oxonol V. As seen in Fig. 8, creation of $\Delta\psi$ did not have any significant effect on the anisotropy decay behavior in both the cases. The small changes observed could be due to $\Delta\psi$-induced shift in the population levels as seen in fluorescence lifetime measurements. The anisotropy did not decay back to zero as seen from the smooth simulated lines in Fig. 8. The values of r_∞ were 0.10 and 0.206 for $diOC_2(5)$ and oxonol V, respectively. The nonzero values of r_∞ would arise from restricted motion of the bound dye. This suggests that oxonol V is bound more firmly compared with $diOC_2(5)$.

DISCUSSION

It is generally recognized that the distribution of fluorophore in bilayers is not likely to be homogeneous, in the sense that the properties of the fluorophores are not like those in an isotropic medium. Very little work has been done to quantify the inhomogeneous distribution. For

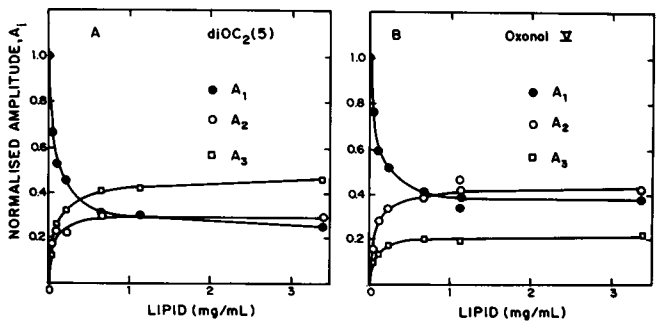

FIGURE 5 Dependence of normalized amplitudes (preexponential factors) associated with fluorescence decay time constants (Table 1) on the concentration of lipid for $diOC_2(5)$ (*A*) and oxonol V (*B*).

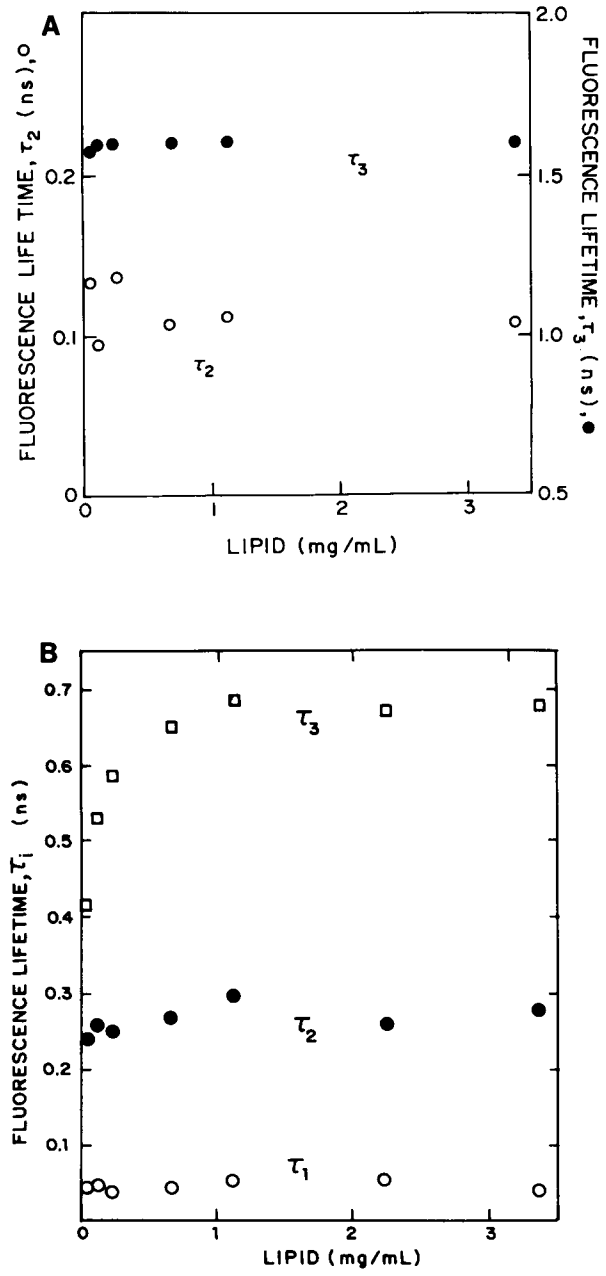

FIGURE 6 Dependence of fluorescence lifetimes of $diOC_2(5)$ (*A*) and oxonol V (*B*) on the concentration of lipid. In the case of $diOC_2(5)$, one of the lifetimes was fixed at 0.65 ns in the analysis.

this reason there has been a lot of discussion concerning the analysis of fluorescence decay of fluorophores in membranes (36–39). A multiexponential function is often used with the understanding that each lifetime represents a population of fluorophores. Usually, two or three exponentials are found to be adequate to fit the data. Analysis of the decay curve for a distribution of lifetimes has also been proposed and carried out, although the choice of a distribution function is arbitrary (36–38). Moreover, it has been shown that the discrimination between discrete lifetimes and distribution of lifetimes based on statistical analysis of the data is not always unambiguous (36, 37). Recently, it has been shown that the decay of membrane-bound fluorophore ought to be nonexponential if the membrane fluidity permits reorientation of the dye in excited state (39). It will, however, be difficult to resolve all the details of the complex nature of the decay from experimental data. The two-exponential decay of diphenyl hexatriene in dipalmitoyl phosphatidylcholine bilayers was shown to be consistent with the above theory (39).

The main aim of the present work was to identify the mechanism of the fluorescence response of the dye to $\Delta\psi$

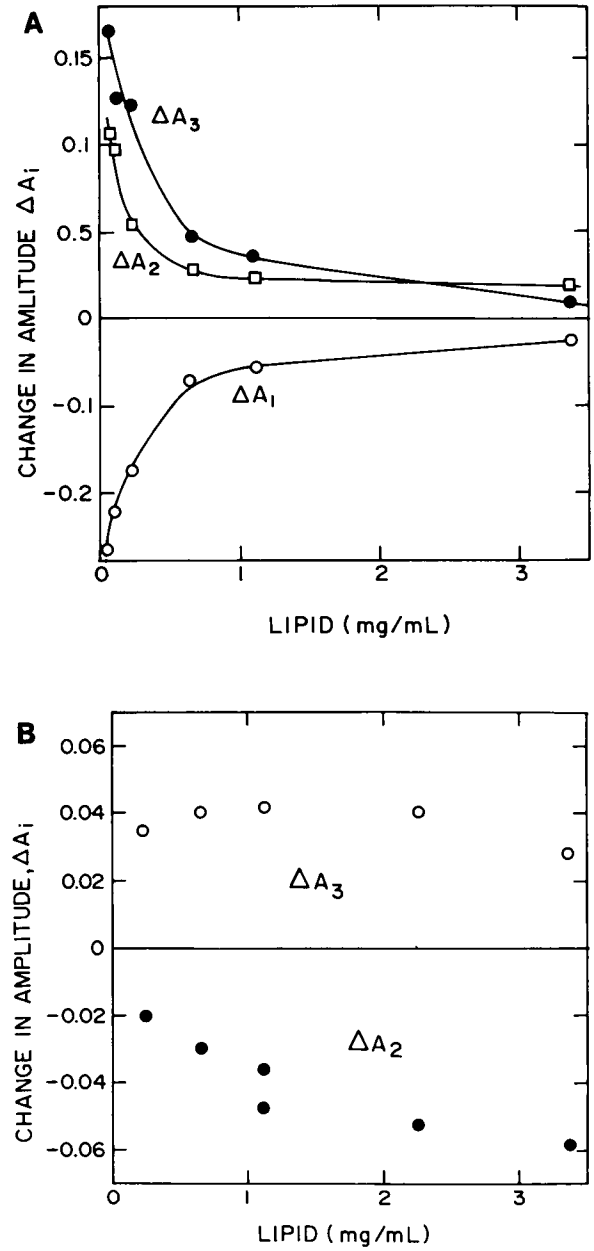

FIGURE 7 Variation of the $\Delta\psi$-induced change in the normalized amplitudes with the concentration of lipid. The sign of $\Delta\psi$ was negative inside for $diOC_2(5)$ (*A*) and positive inside for oxonol V (*B*). In the case of oxonol V, the uncertainty in ΔA_1 was quite large (see text) and hence it is not given.

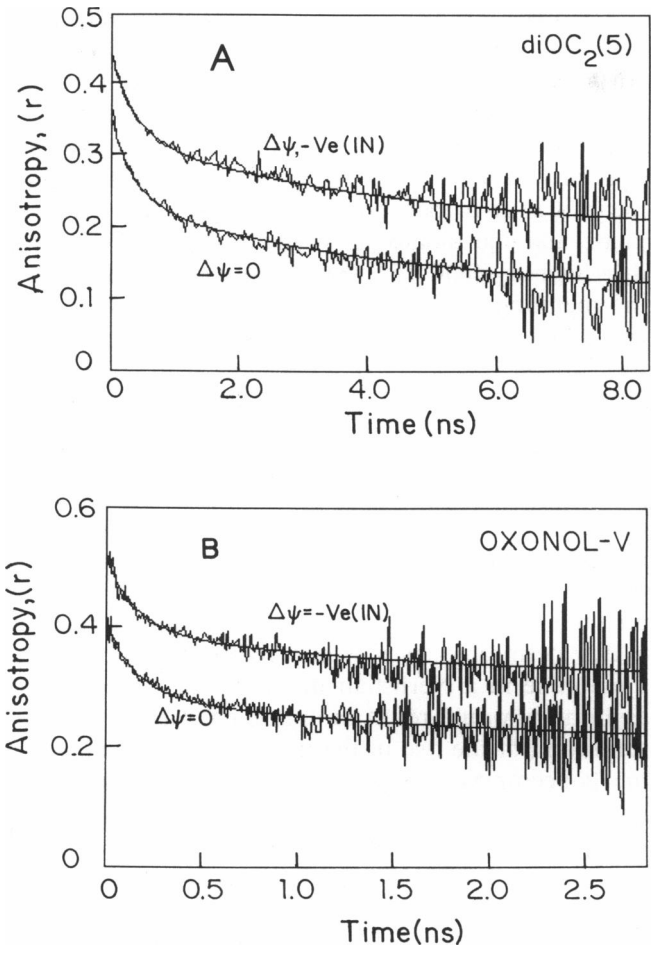

FIGURE 8 Decay of fluorescence anisotropy (r) of $diOC_2(5)$ (A) and oxonol V (B) in liposome suspensions and the effect of $\Delta\psi$ (negative inside). The concentration of lipid was 0.1 mg/ml for A and 1 mg/ml for B. The excitation and emission wavelengths were 575 and 610 nm for A and 600 and 630 nm for B. The top curve ($\Delta\psi$, negative) in both A and B was shifted up by 0.1 to avoid congestion. The smooth lines are simulations of the equation $r(t) = A_1 \exp(-t/\Phi_1) + A_2 \exp(-t/\Phi_2) + r_\infty$ with the values of A_1, A_2, Φ_1, and Φ_2 as 0.117, 0.137, 0.417 ns, and 5.41 ns for A and 0.119, 0.082, 0.17, and 1.99 ns for B. The values of r_∞ were 0.10 for A and 0.206 for B. The smooth lines do not have any theoretical significance.

observed in steady-state experiments. We have uniformly adopted the strategy of fitting the decay curve to three exponentials (two exponentials are inadequate) associated with different populations for the following reasons. (a) The dyes used in this work are water soluble and the dye is distributed between membrane and aqueous phase in most or all of the samples studied by us. (b) In the case of merocyanine 540, a dye structurally similar to the ones used in this work, distribution of the dye in the membrane was found to be heterogeneous (14), where orientation of the dye was parallel or perpendicular to the plane of the membrane. (c) The effect of $\Delta\psi$ is known not to affect the lipid bilayer properties. Otherwise, practically all membrane-soluble dyes could be used to sense $\Delta\psi$ due to the change in the environment of the bound dye. The potential-sensing dyes are usually charged and $\Delta\psi$ interacts with the charge or dipole moment of the dye affecting the physical state of the dye in the membrane. Thus, the existence of at least two bound forms makes sense.

Time-resolved fluorescence of the two typical voltage-sensitive dyes $diOC_2(5)$ and oxonol V in liposome suspensions has been resolved into three components. Comparison of their fluorescence lifetimes with those obtained in the absence of liposomes and titrations with the lipid (Fig. 5) has identified one of the three lifetimes (τ_1) as corresponding to the aqueous population in samples with lipid concentration less than ~1 mg/ml. The other two populations (with lifetimes τ_2 and τ_3) have been identified as membrane-bound forms as seen by the increase in their levels (A_2 and A_3) with increase in the concentration of the lipid (Fig. 5). Beyond ~1 mg/ml of lipid, all the three lifetimes correspond to bound forms. The earlier time-resolved fluorescence study of oxonol V in submitochondrial particles (40) had resolved only two lifetimes, 80 and ~600 ps. In their analysis, the decay curves were not deconvoluted with the excitation pulses. Also, time resolution was achieved using a form of coincidence spectroscopy (40) rather than a more precise time-correlated single photon counting technique used in our work. This could explain our resolution of the decay curves into three exponentials. Two lifetimes (0.3 and 0.7 ns) were reported for the cationic styryl probe in dimyristoylphosphatidyl choline vesicles (41). This was interpreted as due to two different bound forms.

Surprisingly, in the case of $diOC_2(5)$, one of the bound forms (τ_2) had a lifetime of ~0.1 ns (Table 1), which is significantly shorter than the lifetime of the free dye (0.65 ns). The time constant (τ_2) of ~0.1 ns may be the result of the excited state of a bound form (say, D_{b1}) getting transformed into another population (say, D_{b2})

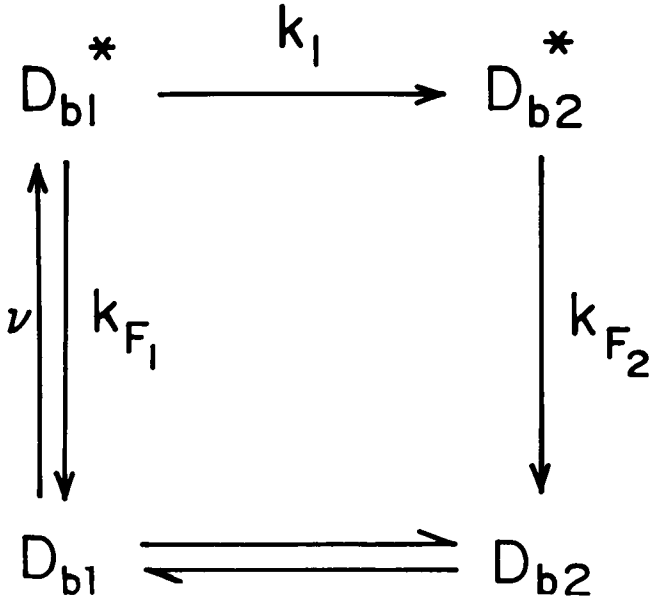

having a lower or negligible quantum yield at the wavelength of observation (scheme 1). The driving force for such a transformation could be a charge-shift generated by excitation (21–23). In this model, τ_2 will be a function of both the rate of decay of fluorescence from D_{b1} and the rate of transformation of D_{b1} into D_{b2}. The similar dependence of A_1 and A_2 on the emission wavelength (data not shown) suggests that the environment of the population D_{b1} is similar to that of the aqueous dye. This could indicate the location of D_{b1} to be at the membrane–water interface. In this model also, the relative changes in A_2 will be proportional to the changes in the concentration of that bound form.

In contrast to the observations in $diOC_2(5)$, the lifetimes of the three bound forms of oxonol V (at lipid concentrations > 0.3 mg/ml) were ~50, ~0.3, and ~0.6 ns. The last two lifetimes are very much longer than the lifetime of aqueous oxonol V (50 ps). Because the resolution of our technique is ~10–20 ps, any other shorter lifetime could not have shown up.

Nonfluorescent dye aggregates are not formed either in the aqueous phase or in the membrane phase, as seen by the following observations. The steady-state fluorescence intensity of the dyes varied linearly with respect to their concentration in the aqueous medium (data not shown) under our sample conditions, thus eliminating nonfluorescent dye aggregates in aqueous solutions. Also, the total fluorescence intensity did not change significantly with the increase in the lipid concentration beyond ~1 mg/ml (the concentration at which the binding to membranes is essentially complete, see Fig. 5) as shown in Fig. 2. This rules out any significant level of nonfluorescent dye aggregates in the membrane. The very low concentrations of the dye used in our samples ([dye]/[liposome] ~ 1 or less) are highly unlikely to have caused aggregates in the membrane phase.

Our aim in this work was to identify the correct model to explain the mechanism of response of these dyes (see Introduction). Our data (Table 1 and Fig. 7 *A*) show clearly that $\Delta\psi$ perturbs the equilibrium between the aqueous (τ_1) and membrane-bound (τ_2 and τ_3) dye population in the case of $diOC_2(5)$. An inside negative $\Delta\psi$ shifts the equilibrium in favor of the bound form of the positively charged $diOC_2(5)$. This is a clear evidence in favor of the "on–off" mechanism. Although a similar conclusion had been derived in earlier work based on steady-state fluorescence measurements (18, 19), the results were always associated with uncertainty arising from spectral overlaps of free and bound dye populations. Our data are also unambiguous in showing that there is no significant $\Delta\psi$-induced shift in equilibria between bound forms of $diOC_2(5)$. This was shown by the changes in amplitudes A_2 and A_3 (Table 1 and Fig. 7 *A*). This conclusion is stronger from data with high concentrations of the lipid where most of the dye is membrane bound (Fig. 7 *A*).

Although the term "on–off" encompasses mechanisms involving $\Delta\psi$-dependent partitioning between the aqueous and the membrane phase, the actual mechanism could depend upon whether or not the dye is membrane permeable. In the case of charged and impermeant dyes such as WW781, the "on–off" mechanism would mean a shift in partition between the outer aqueous phase and the membrane–water interface. Permeable dyes such as $diOC_2(5)$ would easily equilibrate across the membrane. Hence a $\Delta\psi$-induced "on–off" occurring at one side of the membrane would be cancelled by the "on–off" signal of opposite sign at the other side. However, we observed $\Delta\psi$-induced fluorescence changes in liposome preparations having identical concentrations of $diOC_2(5)$ in both inner and outer aqueous compartments (data not shown). The magnitude of the signal was comparable to that observed in samples where the dye was added only to the outer medium. It is likely that the large ratio of the volumes of the two aqueous phases is responsible for the net signal change. Driven by a $\Delta\psi$, permeable dyes would redistribute across the membrane in a Nernstian manner. The large volume asymmetry would result in drastic changes in the concentration of the dye in the inner compartment, while the concentration in the outer phase would remain largely unaltered. If there is equilibrium between free and bound forms at each side of the membrane, a change in the concentration in the inner phase would change the amount of the inner bound form (5). In this mechanism, the dependence of the partition coefficient on $\Delta\psi$ manifests through a Nernstian distribution across the membrane.

In contrast to $diOC_2(5)$, oxonol V responds mainly by a mechanism by which $\Delta\psi$ perturbs the equilibrium between two bound forms (represented by τ_2 and τ_3 of ~0.3 and ~0.6 ns, respectively). An inside positive $\Delta\psi$ increases the relative population of the bound form, with a longer lifetime resulting in increase in the overall fluorescence intensity. The different populations could represent oxonol V in different locations in the membrane. The shortest component (τ_1) could arise from either free oxonol V (at lipid concentrations below ~0.3 mg/ml) or bound oxonol V at the membrane–water interface (at lipid concentrations above ~0.3 mg/ml). The two longer components could represent dye populations buried (to different extents) in the hydrophobic core of the bilayer. Multiple location of some oxonols in bilayers have been suggested earlier (20). Because an inside positive $\Delta\psi$ increased the relative population of the τ_3 component (and the reverse for an inside negative $\Delta\psi$), this population could be more buried compared with the populations represented by either τ_1 or τ_2. One could expect the $\Delta\psi$-induced shift in the equilibrium taking place at one side of the bilayer to cancel the shift happening at the other side, resulting in zero signal. However, the high asymmetry in the area of the two monolayers in small

(~300-Å diam; reference 26) vesicles is expected to result in a net signal change, as experimentally obtained. Changes taking place at the outer monolayer will be dominant.

The different mechanisms of response by the two dyes as inferred from our fluorescence lifetime measurements get support from the steady-state measurements (Fig. 2, *A* and *B*), which show distinct differences in the lipid concentration dependence of signal change ($\Delta F/F$). Furthermore, time-resolved anisotropy decay measurements (Fig. 8) also suggest that oxonol V is bound more firmly compared with $diOC_2(5)$ and hence it is unlikely to show an "on–off" mechanism. The origin of the difference in the mechanism of response of the two dyes is not clear. Difference in the lipophilicity of the two dyes could be a possible reason.

Received for publication 10 September 1992 and in final form 2 December 1992.

REFERENCES

1. Waggoner, A. 1976. Optical probes of membrane potential. *J. Membr. Biol.* 27:317–334.
2. Waggoner, A. S. 1979. Dye indicators of membrane potential. *Annu. Rev. Biophys. Bioeng.* 8:47–68.
3. Ross, W. N., B. M. Salzberg, L. B. Cohen, A. Grinvald, H. V. Davila, A. S. Waggoner, and C. H. Wang. 1977. Changes in absorption, fluorescence, dichroism, and birefringence in stained giant axons: optical measurement of membrane potential. *J. Membr. Biol.* 33:141–183.
4. Singh, A. P., and P. Nicholls. 1985. Cyanine and safranine dyes as membrane potential probes in cytochrome c oxidase reconstituted proteoliposomes. *J. Biochem. Biophys. Methods.* 11:95–108.
5. Apell, H.-J., and B. Bersch. 1987. Oxonol VI as an optical indicator for membrane potentials in lipid vesicles. *Biochim. Biophys. Acta.* 903:480–494.
6. Freedman, J. C., and P. C. Laris. 1988. Optical potentiometric indicators for nonexcitable cells. *In* Spectroscopic Membrane Probes. Vol. 3. L. Loew, editor. CRC Press, Boca Raton, FL. 1–49.
7. Freedman, J. C., and T. S. Novak. 1989. Optical measurements of membrane in cells, organelles and vesicles. *Methods Enzymol.* 172:102–122.
8. Montana, V., D. L. Farkas, and L. M. Loew. 1989. Dual-wavelength ratiometric fluorescence measurements of membrane potential. *Biochemistry.* 28:4536–4539.
9. Smith, J. C. 1990. Potential-sensitive molecular probes in membranes of bioenergetic relevance. *Biochim. Biophys. Acta.* 1016:1–28.
10. Reers, M., T. W. Smith, and L. Bo Chen. 1991. J-aggregate formation of a carbocyanine as a quantitative fluorescent indicator of membrane potential. *Biochemistry.* 30:4480–4486.
11. Tran, T. V., S. Allen, and J. C. Smith. 1991. The behavior of a fast-responding barbituric acid potential-sensitive molecular probe in bovine heart submitochondrial particles. *Biochim. Biophys. Acta.* 1059:265–274.
12. Waggoner, A. S., and A. Grinvald. 1977. Mechanism of rapid optical changes of potential sensitive dyes. *Ann. NY Acad. Sci.* 303:217–241.
13. Waggoner, A. S., C. H. Wang, and R. L. Tolles. 1977. Mechanism of potential-dependent light absorption changes of lipid bilayer membranes in the presence of cyanine and oxonol dyes. *J. Membr. Biol.* 33:109–140.
14. Dragsten, P. R., and W. W. Webb. 1978. Mechanism of the membrane potential sensitivity of the fluorescent membrane probe merocyanine 540. *Biochemistry.* 17:5228–5240.
15. Smith, J. C., S. J. Frank, C. L. Bashford, B. Chance, and B. Rudkin. 1980. Kinetics of the association of potential-sensitive dyes with model and energy-transducing membranes: implications for fast probe response times. *J. Membr. Biol.* 54:127–139.
16. Verkman, A. S., and M. P. Frosch. 1985. Temperature-jump studies of merocyanine 540 relaxation kinetics in lipid bilayer membranes. *Biochemistry.* 24:7117–7122.
17. Cabrini, G., and A. S. Verkman. 1986. Mechanism of interaction of the cyanine dye $DiS\text{-}C_3\text{-}(5)$ with renal brush-border vesicles. *J. Membr. Biol.* 90:163–175.
18. Cabrini, G., and A. S. Verkman. 1986. Potential-sensitive response mechanism of $DiS\text{-}C_3\text{-}(5)$ in biological membranes. *J. Membr. Biol.* 92:171–182.
19. George, E. B., P. Nyirjesy, M. Basson, L. A. Ernst, P. R. Pratap, J. C. Freedman, and A. S. Waggoner. 1988. Impermeant potential-sensitive oxonol dyes. I. Evidence for an "on–off" mechanism. *J. Membr. Biol.* 103:245–253.
20. Pratap, P. R., T. S. Novak, and J. C. Freedman. 1990. Two mechanisms by which fluorescent oxonols indicate membrane potential in human red blood cells. *Biophys. J.* 57:835–849.
21. Loew, L. M., G. W. Bonneville, and J. Surow. 1978. Charge shift optical probes of membrane potential. Theory. *Biochemistry.* 17:4065–4071.
22. Loew, L. M., S. Scully, L. Simpson, and A. S. Waggoner. 1979. Evidence for a charge-shift electrochromic mechanism in a probe of membrane potential. *Nature (Lond.).* 281:497–499.
23. Fluhler, E., V. G. Burnham, and L. M. Loew. 1985. Spectra, membrane binding, and potentiometric responses of new charge shift probes. *Biochemistry.* 24:5749–5755.
24. Chance, B., and M. Baltscheffsky, with an appendix by W.-K. Cheng. 1975. Carotenoid and merocyanine probes in chromatophore membranes. *In* Biomembranes. Vol. 7. H. Eisenberg, E. Katchalski-Katzir, and L. A. Mason, editors. Plenum Publishing Corp., New York. 33–59.
25. Cooper, C. E., D. Bruce, and P. Nicholls. 1990. Use of oxonol V as a probe of membrane potential in proteoliposomes containing cytochrome oxidase in the sub-mitochondrial orientation. *Biochemistry.* 29:3859–3865.
26. Krishnamoorthy, G. 1986. Temperature jump as a new technique to study the kinetics of fast transport of protons across membranes. *Biochemistry.* 25:6666–6671.
27. Periasamy, N., S. Doraiswamy, G. B. Maiya, and B. Venkataraman. 1988. Diffusion controlled reactions: fluorescence quenching of cationic dyes by charged quenchers. *J. Chem. Phys.* 88:1638–1651.
28. Banker, K. V., V. R. Bhagat, R. Das, S. Doraiswamy, A. S. Ghangrekar, D. S. Kamat, N. Periasamy, V. J. P. Srivatsavoy, and B. Venkataraman. 1989. Techniques for the study of fast chemical processes with half-times of the order of microseconds or less. *Indian J. Pure Appl. Phys.* 27:416–428.
29. Bevington, P. R. 1969. *In* Data Reduction and Analysis in Physical Sciences. McGraw-Hill Inc., New York. 204–246.
30. Knutson, J. R., J. M. Beechem, and L. Brand. 1983. Simultaneous analysis of multiple fluorescence decay curves: a global approach. *Chem. Phys. Lett.* 102:501–507.
31. Kragh-Hansen, U., K. E. Jorgensen, and M. I. Sheikh. 1982. The

use of a potential-sensitive cyanine dye for studying ion-dependent electrogenic renal transport of organic solutes. Uptake of L-malate and D-malate by luminal-membrane vesicles. *Biochem. J.* 208:369–376.

32. Yoshikami, D., and L. M. Okun. 1984. Staining of living presynaptic nerve terminals with selective fluorescent dyes. *Nature (Lond.).* 310:53–56.
33. Oseroff, A. R., D. Ohuoha, G. Ara, D. McAuliffe, J. Foley, and L. Cincotta. 1986. Intramitochondrial dyes allow selective in vitro photolysis of carcinoma cells. *Proc. Natl. Acad. Sci. USA.* 83:9729–9733.
34. Alcover, A., M. J. Weiss, J. F. Daley, and E. L. Reinherz. 1986. The T11 glycoprotein is functionally linked to a calcium channel in precursor and mature T-lineage cells. *Proc. Natl. Acad. Sci. USA.* 83:2614–2618.
35. Ehrenberg, B., V. Montana, M.-D. Wei, and J. P. Wuskell. 1988. Membrane potential can be determined in individual cells from the Nernstian distribution of cationic dye. *Biophys. J.* 53:785–794.
36. James, D. R., and W. R. Ware. 1985. The photophysics of homotryptophan. *Chem. Phys. Lett.* 120:450–454.
37. James, D. R., J. R. Turnbull, B. D. Wagner, W. R. Ware, and N. O. Peterson. 1987. Distribution of fluorescence decay times for parinaric acids in phospholipid membranes. *Biochemistry.* 26:6272–6277.
38. Kalb, E., F. Paltauf, and A. Hermetter. 1986. Fluorescence lifetime distributions of diphenylhexatriene-labeled phosphatidylcholine as a tool for the study of phospholipid–cholesterol interactions. *Biophys. J.* 56:1245–1253.
39. Toptygin, J., J. Svobodova, I. Konopasek, and L. Brand. 1992. Fluorescence decay and depolarization in membranes. *J. Chem. Phys.* 96:7919–7930.
40. Smith, J. C., L. Hallidy, and M. R. Topp. 1981. The behavior of the fluorescence lifetime and polarization of oxonol potential-sensitive extrinsic probes in solution and in beef heart submitochondrial particles. *J. Membr. Biol.* 60:173–185.
41. Bammel, B. P., D. D. Hamilton, R. P. Haugland, H. P. Hopkins, J. Schuette, W. Szalecki, and J. C. Smith. 1990. NMR, calorimetric, spin-label, and optical studies on a trifluoro-methyl substituted styryl molecular probe in dimyristoylphosphatidylcholine vesicles and multilamellar suspensions: a model for location of optical probes. *Biochim. Biophys. Acta.* 1024:61–81.